A NUMERICAL INVESTIGATION OF TURBULENT BOUNDARY LAYER DETACHMENT AT AN ASYMMETRIC STRAIGHT-WALLED DIFFUSER

Rafael Gabler Gontijo, rafaelgabler@yahoo.com.br
José Luiz Alves da Fontoura Rodrigues, fontoura@unb.br
Universidade de Brasília, Departamento de Engenharia Mecânica, 70910-900, Brasília - DF
Daniel Vieira Soares, danielvs@ufrj.br
Universidade Federal do Rio de Janeiro, Programa de Engenharia Mecânica/COPPE, 21945-970, Rio de Janeiro - RJ

Abstract. *This works shows how some technicalities in the design of the diffuser can affect the turbulent boundary layer detachment. The behavior of a turbulent flow of air, inside a two dimensional asymmetric straight-walled diffuser, with an divergence angle of 9.97 degrees, is numerically simulated considering some aspects of the solid boundary geometry. The velocity profiles and the recirculation regions are compared with the experimental data. The research algorithm used to simulate the turbulent flow applies a consolidate Reynolds averaging process for the turbulent variables and uses the classical $\kappa-\varepsilon$ model. The turbulent inner layer is modeled by four distinct velocity laws of the wall. Spacial discretization is done by a finite element method and temporal discretization is implemented using a semi-implicit sequential scheme of finite differences. The pressure-velocity coupling is numerically solved by a variation of Uzawa's algorithm. To filter the numerical noises, originated by the symmetric treatment given to the convective fluxes, it is adopted a balance dissipation method. The remaining non-linearities, due to laws of the wall explicit calculation, are treated by a minimal residual method.*

Keywords: *turbulence, laws of the wall, boundary layer detachment, adverse pressure gradient, straight-walled diffuser*

1. INTRODUCTION

In the last three decades great amount of research has been done in the numerical simulation of turbulent flows, with emphasis on turbulent flows of industrial and environmental interest. In this work we bring into prominence the detachment of turbulent boundary layer, induced by smooth adverse pressure gradients, like happens inside a straight-walled diffuser with a divergence angle of 9.97 degrees. The diffusers are a geometry of particular interest due to its great importance in the behavior of a wide diversity of machines.

To avoid the boundary layer detachment in a diffuser is a vital task to assure it's main purpose: to convert as large a fraction as possible of the dynamic pressure into static pressure. The straight way to prevent the boundary layer detachment is to design a diffuser with a small divergence angle but, in order to achieve a high static pressure, the size of the diffuser axial length would be necessarily large, which is a handicap. However, numerical results presented in this work, strongly suggest that constructive details, in the inlet and outlet of the diffuser, are capable of increasing locally the turbulent intensity and may act decreasing or, at least, preventing the boundary layer detachment inside the diffuser. If experimental results confirm what is observed in the numerical simulation, this feature of turbulent flows in plane diffusers could be studied in a broader way, with the goal of normalizing very cheap and simple constructive procedures, capable to difficult or, at a limitrophe circumstance, to avoid the boundary layer detachment inside diffusers.

The constructive detail mentioned is the curvature in the inlet and on the outlet of the diffuser, as detailed by Buice and Eaton (1995). This work observed numerically that when the transition between the entering channel and the diffuser is conducted by a smooth curvature, the boundary layer detachment is increased for small divergence angles. When the transition is done directly, without considering a smooth curvature, the boundary layer detachment is decreased. The reasons for this behavior will be discussed still.

This work does a numerical analysis about the influence of the geometry details in the dynamic field of a turbulent flow of air, inside an asymmetric straight-walled diffuser with an divergence angle of 9.97 degrees. The numerical results of this work are confronted with the experimental data obtained by Buice and Eaton (1995).

The solver used, named Turbo2D, is a research Fortran numerical code, that has been continuously developed by members of the Group of Complex Fluid Dynamics - Vortex, of the Mechanical Engineering Department of the University of Brasília, in the last twenty years. This solver is based on the adoption of the finite elements technique, under the formulation of weighted residuals proposed by Galerkin, adopting in the spatial discretization of the calculation domain the triangular elements of the type P1 and P1-isoP2, as proposed by Brison, Buffat, Jeandel and Serres (1985). In the P1 mesh only the pressure field is calculated while all the other variables are calculated in the P1-isoP2 mesh.

Considering the uncertainties normally existing about the initial conditions of the flow to be simulated, it is adopted the temporal integration of the governing equations system. In the temporal integration process, at the beginning of the flow, the initial state corresponds to an arbitrary value of all dependent variables and the final state is attained when are concluded the temporal variations of the velocity, pressure, density and other turbulent variables. The temporal discretization of the of the governing equations system, implemented by the algorithm of Brun (1988), uses sequential semi-implicit finite differences, with truncation error of order $0(\Delta t)$ and allows a linear handling of the equation system, at each time step.

The resolution of the coupled equations of continuity and momentum is done by a variant of Uzawa's algorithm proposed by Buffat (1981). The statistical formulation, responsible for the obtaining of the system of average equations, is done with the simultaneous usage of the Reynolds (1895) and Favre (1965) decomposition. The Reynolds stress tensor is calculated by the $\kappa - \varepsilon$ model, proposed by Jones and Launder (1972) with the modifications introduced by Launder and Spalding (1974).

In the program Turbo2D, the boundary conditions of velocity can be calculated by four velocity laws of the wall. The velocity laws of the wall used in this work are: the classical logarithm law, and the laws of Mellor (1966), Nakayama and Koyama (1984), and Cruz and Silva Freire (1998). The numerical instability resultant of the explicit calculation of the boundary conditions of velocity, through the evolutive temporal process, is controlled by the algorithm proposed by Fontoura Rodrigues (1990). The numerical oscillations induced by the Galerkin formulation, resulting of the centered discretization applied to a parabolic phenomenon, that is the modeled flow, are cushioned by the technique of balanced dissipation, proposed by Huges and Brooks (1979) and Kelly, Nakazawa and Zienkiewicz (1976) with the numerical algorithm proposed by Brun (1988).

In order to quantify the wideness of range and the consistence of the numerical modeling done by the solver Turbo2D, the results obtained numerically are compared to the experimental data of Buice and Eaton (1995).

2. Governing equations

The turbulent one phase flow analyzed in the present work is homogeneous, at low Mach number, and the gravitational force is small compared to advective effects. Considering the procedures shown by Soares and Fontoura Rodrigues (2004), with pertinent adaptations for isothermal flows, the conservation equations of mass and momentum, which des-cribe the phenomena, are respectively represented, in Einstein's notation, by the dimensionless relations:

$$\frac{\partial u_i}{\partial x_i} = 0 \ , \tag{1}$$

$$\frac{\partial u_i}{\partial t} + u_j \frac{\partial u_i}{\partial x_j} = -\frac{1}{\rho}\frac{\partial p}{\partial x_i} + \frac{1}{Re}\frac{\partial}{\partial x_j}\left(\frac{\partial u_i}{\partial x_j} + \frac{\partial u_j}{\partial x_i}\right) \ , \tag{2}$$

where ρ is the fluid density, t represents time, x_i a cartesian coordinate, u_i is the i^{th} velocity component, p is the thermodynamic pressure and Re is the Reynolds number.

2.1 The turbulence model

The adopted methodology is a transformation of the system of instantaneous dimensionless governing equations into a system of mean equations, obtained using a statistical treatment, resultant from the Reynolds averaging.

The closure of the mean equations is based on Boussinesq's (1877) hypothesis of eddy viscosity. For the velocity fluctuation correlation tensor, the Reynolds Stress Tensor, takes the form:

$$\overline{u_i'' u_j''} = \frac{2}{3}\kappa\delta_{ij} - \nu_t\left(\frac{\partial \overline{u}_i}{\partial x_j} + \frac{\partial \overline{u}_j}{\partial x_i}\right) \ , \tag{3}$$

where ν_t is the eddy viscosity, κ is the turbulent kinetic energy, δ_{ij} is the delta of Kronecker operator and the over-bars indicate averaged variables. The form adopted in this work to express the eddy viscosity ν_t, as a function of the turbulent kinetic energy κ and its dissipation rate ε, is using the Prandtl - Kolmogorov relation:

$$\nu_t = C_\mu \frac{\kappa^2}{\varepsilon} = \frac{1}{Re_t} \qquad \text{and} \tag{4}$$

where C_μ is a constant of value 0.09. With the adoption of relation (4), the $\kappa - \varepsilon$ turbulence model relation imposes the necessity of two supplementary transport equations to the system of mean equations, destined to evaluation of variables κ and ε. Once defined the closure of the mean equations system, the direction proposed by Brun (1988) produces the following system of equations:

$$\frac{\partial \overline{u}_i}{\partial x_i} = 0 \ , \tag{5}$$

$$\frac{\partial \overline{u}_i}{\partial t} + \overline{u}_j \frac{\partial \overline{u}_i}{\partial x_j} = -\frac{1}{\rho}\frac{\partial \overline{p^*}}{\partial x_i} + \frac{\partial}{\partial x_j}\left[\left(\frac{1}{Re} + \frac{1}{Re_t}\right)\left(\frac{\partial \overline{u}_i}{\partial x_j} + \frac{\partial \overline{u}_j}{\partial x_i}\right)\right] \ , \tag{6}$$

$$\frac{\partial \kappa}{\partial t} + \overline{u}_i \frac{\partial \kappa}{\partial x_i} = \frac{\partial}{\partial x_i}\left[\left(\frac{1}{Re} + \frac{1}{Re_t\,\sigma_\kappa}\right)\frac{\partial \kappa}{\partial x_i}\right] + \Pi - \varepsilon \ , \tag{7}$$

$$\frac{\partial \varepsilon}{\partial t} + \overline{u}_i \frac{\partial \varepsilon}{\partial x_i} = \frac{\partial}{\partial x_i}\left[\left(\frac{1}{Re} + \frac{1}{Re_t\,\sigma_\varepsilon}\right)\frac{\partial \varepsilon}{\partial x_i}\right] + \frac{\varepsilon}{\kappa}\left(C_{\varepsilon 1}\Pi - C_{\varepsilon 2}\varepsilon\right) \ , \tag{8}$$

where:

$$\Pi = \left[\left(\frac{1}{Re_t}\right)\left(\frac{\partial \overline{u}_i}{\partial x_j} + \frac{\partial \overline{u}_j}{\partial x_i}\right) - \frac{2}{3}\kappa\delta_{ij}\right]\frac{\partial \overline{u}_i}{\partial x_j} \ , \tag{9}$$

$$p^* = \bar{p} + \frac{2}{3}\rho\kappa \ , \tag{10}$$

and the constants of the model are given:

$$C_\mu = 0.09\ ,\ C_{\varepsilon 1} = 1.44\ ,\ C_{\varepsilon 2} = 1.92\ ,\ \sigma_\kappa = 1\ ,\ \sigma_\varepsilon = 1.3\ . \tag{11}$$

2.2 NEAR WALL TREATMENT

The $\kappa - \varepsilon$ turbulence model is incapable of properly representing the laminar sub-layer and the transition regions of the turbulent boundary layer. To solve this inconvenience, the solution adopted in this work are the laws of the wall for velocity employment, capable of properly representing the flow in the inner region of the turbulent boundary layer.

There are four velocity laws of the wall implemented on Turbo 2D. The laws used in this simulation are shown bellow, except for the classical log law, that further explanations are unnecessary.

2.2.1 Velocity law of the wall of Mellor (1966)

Deduced from the mean equation of Prandtl for the turbulent boundary layer, considering the pressure gradient term for integration, this wall function is a primary approach to flows that suffer influence of adverse pressure gradients. Its equations are, respectively, for the laminar and turbulent region

$$u^* = y^* + \frac{1}{2}p^* y^{*2} \ , \tag{12}$$

$$u^* = \frac{2}{K}\left(\sqrt{1 + p^* y^*} - 1\right) + \frac{1}{K}\left(\frac{4y^*}{2 + p^* y^* + 2\sqrt{1 + p^* y^*}}\right) + \xi_{p^*} \ , \tag{13}$$

where the asterisk upper-index indicates dimensionless quantities of velocity u^*, pressure gradient p^* and distance to the wall y^*, as functions of scaling parameters to the near wall region, K is the Von Karman constant, and ξ_{p^*} is Mellor's integration constant, function of the near-wall dimensionless pressure gradient, determined in his work of 1966.

The intersection of both regions is considered to be the same as the log law expressions, with $y^* = 11,64$. The relations between the dimensionless near wall properties and the friction velocity u_f are:

$$y^* = \frac{y\,u_f}{\nu} \quad , \quad u^* = \frac{\widetilde{u}_x}{u_f} \quad \text{and} \quad p^* = \frac{1}{\bar{\rho}}\frac{\partial \bar{p}}{\partial x}\frac{\nu}{{u_f}^3} \ . \tag{14}$$

The friction velocity is calculated by the relation:

$$u_f = \left(\frac{1}{Re} + \frac{1}{Re_T}\right)\frac{\partial u_i}{\partial x_j} - \frac{1}{\rho}\frac{\partial P}{\partial x_i}\delta_{ij} \tag{15}$$

In equation (13) the term ξ_{p^*} is a value obtained from the integration process proposed by Mellor (1966) and is a function of the dimensionless pressure gradient. Its values are obtained through interpolation of those obtained experimentally by Mellor, shown in Tab. 1.

Table 1. Mellor's integration constant (1966)

p^*	-0.01	0.00	0.02	0.05	0.10	0.20	0.25	0.33	0.50	1.00	2.00	10.00
ξ_{p^*}	4.92	4.90	4.94	5.06	5.26	5.63	5.78	6.03	6.44	7.34	8.49	12.13

2.2.2 Velocity law of the wall of Nakayama and Koyama (1984)

In their work, Nakayama and Koyama (1984) proposed a derivation of the mean turbulent kinetic energy equation, that resulted in an expression to evaluate the velocity near solid boundaries. Using experimental results and those obtained by Strattford (1959), the derived equation is

$$u^* = \frac{1}{K^*}\left[3(t-t_s) + ln\left(\frac{t_s+1}{t_s-1}\frac{t-1}{t+1}\right)\right] \quad , \tag{16}$$

with

$$t = \sqrt{\frac{1+2\tau^*}{3}} \quad , \quad \tau^* = 1 + p^* y^* \quad , \quad K^* = \frac{0,419 + 0,539p^*}{1+p^*} \quad and \quad {y^*}_s = \frac{e^{K\ C}}{1+p^{*0,34}} \ , \tag{17}$$

where K^* is the expression for the Von Karman constant modified by the presence of adverse pressure gradients, τ^* is a dimensionless shear stress, $C = 5.445$ is the log-law constant and t, ${y^*}_s$ and t_s, a value of t at position ${y^*}_s$, are parameters of the function.

2.2.3 Velocity law of the wall of Cruz and Silva Freire (1998)

Analyzing the asymptotic behavior of the boundary layer flow under adverse pressure gradients, Cruz and Silva Freire (1998) derived an expression for the velocity. The solution of the asymptotic approach is

$$u = \frac{\tau_w}{|\tau_w|}\frac{2}{K}\sqrt{\frac{\tau_w}{\rho} + \frac{1}{\rho}\frac{dp_w}{dx}y} + \frac{\tau_w}{|\tau_w|}\frac{u_f}{K}ln\left(\frac{y}{L_c}\right) \quad with \quad L_c = \frac{\sqrt{\left(\frac{\tau_w}{\rho}\right)^2 + 2\frac{\nu}{\rho}\frac{dp_w}{dx}u_f} - \frac{\tau_w}{\rho}}{\frac{1}{\rho}\frac{dp_w}{dx}} \ , \tag{18}$$

where the sub-index $_w$ indicates the properties at the wall, K is the Von Karman constant, L_c is a length scale parameter and u_f is the friction velocity.

The proposed equation for the velocity, equation (18), has a behavior similar to the log law far from the separation and retachment points, but close to the separation point, it gradually tends to Stratford's equation (1959).

3. NUMERICAL METHODOLOGY

The numerical solution of a turbulent wall flow, with the heigh Reynolds $\kappa - \varepsilon$ turbulence model used in this work, has as main difficulties the coupling between all equations; the non-linear behavior resulting of the simultaneous action of advective and eddy viscosity terms; the explicit calculations of boundary conditions in the solid boundary and the methodology of use the continuity equation as a manner to link the coupled fields of velocity and pressure.

The solution proposed in the present work suggests a temporal discretization of the system of governing equations with a sequential semi-implicit finite difference algorithm proposed by Brun (1988) and a spatial discretization using finite elements of the type P1-isoP2. The temporal and spatial discretization implemented in Turbo 2D is presented in Fontoura Rodrigues (1990).

3.1 Numerical solver algorithm

The system of governing equations is spatially discretized using a first order approximation to the temporal derivative, obtained with a sequential semi-implicit finite difference algorithm, with first order truncating error, which allows a complete linearization of all equations at each time step. The algorithm proposed by Brun (1988) starts the calculation with a known field at an instant $n\Delta t$, calculating the momentum, the pressure, the temperature, the density, the turbulence kinetic energy and its dissipation rate at an instant $(n+1)\Delta t$, where n is a integer number and Δt is a time interval, by means of a sequence of calculations divided in three stages.

On the first stage, the boundary conditions at an instant $(n+1)\Delta t$ for the velocity field are obtained from a chosen law of the wall, using values from instant $n\Delta t$. On the second stage, the fields of momentum and pressure are calculated at instant $(n+1)\Delta t$, using a variation of Uzawa's minimum residuals algorithm proposed by Buffat (1981), with the coupled system of equations:

$$\frac{\partial {\overline{u}_i}^{n+1}}{\partial x_i} = 0 \ , \tag{19}$$

$$\begin{aligned} \frac{{\overline{u}_i}^{n+1} - {\overline{u}_i}^{n}}{\Delta t} + {\overline{u}_j}^{n}\frac{\partial {\overline{u}_i}^{n+1}}{\partial x_j} &= -\frac{1}{\rho}\frac{\partial \bar{p^*}^{n+1}}{\partial x_i} \\ &+ \frac{\partial}{\partial x_j}\left[\left(\frac{1}{Re} + \frac{1}{{Re_t}^n}\right)\left(\frac{\partial {\overline{u}_i}^{n+1}}{\partial x_j} + \frac{\partial {\overline{u}_j}^{n+1}}{\partial x_i}\right)\right] . \end{aligned} \tag{20}$$

On the third and last stage, all other variables are solved at instant $(n+1)\Delta t$:

$$\begin{aligned}
\frac{\kappa^{n+1}-\kappa^n}{\Delta t} + \overline{u}_j{}^n \frac{\partial \kappa^{n+1}}{\partial x_j} &= +\frac{\partial}{\partial x_j}\left[\left(\frac{1}{Re}+\frac{1}{Re_t{}^n\,\sigma_\kappa}\right)\left(\frac{\partial \kappa^{n+1}}{\partial x_j}\right)\right] \\
&\quad +\Pi^{n+1} - \frac{\varepsilon^n}{\kappa^n}\kappa^{n+1} \quad , \qquad (21)\\
\frac{\varepsilon^{n+1}-\varepsilon^n}{\Delta t} + \overline{u}_j{}^n \frac{\partial \varepsilon^{n+1}}{\partial x_j} &= +\frac{\partial}{\partial x_j}\left[\left(\frac{1}{Re}+\frac{1}{Re_t{}^n\,\sigma_\varepsilon}\right)\left(\frac{\partial \varepsilon^{n+1}}{\partial x_j}\right)\right] \\
&\quad +\frac{\varepsilon^n}{\kappa^n}\left(C_{\varepsilon 1}\Pi^{n+1} - C_{\varepsilon 2}\varepsilon^{n+1}\right) \quad , \qquad (22)
\end{aligned}$$

with the production term Π and the modified pressure $\bar{p^*}$ given by:

$$\begin{aligned}
\Pi^{n+1} &= \frac{\partial \overline{u}_i^{n+1}}{\partial x_j}\left[\left(\frac{1}{Re_t^n}\right)\left(\frac{\partial \overline{u}_i^{n+1}}{\partial x_j}+\frac{\partial \overline{u}_j^{n+1}}{\partial x_i}\right) - \frac{2}{3}\kappa^n\delta_{ij}\right] \quad , \qquad (23)\\
\bar{p^*}^{n+1} &= \bar{p}^{n+1} + \frac{2}{3}\rho\kappa^{n+1} \quad . \qquad (24)
\end{aligned}$$

At last, the turbulent Reynolds number is updated with the newest values:

$$\frac{1}{Re_t^{n+1}} = C_\mu \frac{(\kappa^{n+1})^2}{\varepsilon^{n+1}} \quad , \qquad (25)$$

and then return to the first step, until the required precision is reached.

As the boundary conditions are calculated explicitly, based on values of the instant $n\Delta t$ to determine the conditions for the instant $(n+1)\Delta t$, a numerical instability inevitably appears. To eliminate this characteristic of the use of laws of the wall, in applications where temporal variations are considered, the minimization residuals technique proposed by Fontoura Rodrigues (1990), that adopts an iterative calculation sequence based on the minimization of the resulting error on the evaluation of the friction velocity, defined for a determined iteration *i* at an instant $(n+1)\Delta t$, as:

$$(ERROR)_i^{n+1} = \left|\left|\left(u_f^2\right)^* - \left(u_f^2\right)_i^{n+1}\right|\right| \quad , \qquad (26)$$

where the double bars indicate the absolute values of the vectors, the value of $(u_f^2)^*$ is obtained with the laws of the wall relation, with values of iteration *i* at instant $(n+1)\Delta t$, and the value of $(u_f^2)_i^{n+1}$ is obtained with a numerical relation of recurrence, from the error minimization algorithm.

4. RESULTS

The calculation domain consists in an asymmetric plane diffuser with an opening angle of 9.97^o. In the inlet experimental profiles of velocity, turbulent kinetic energy and its rate of dissipation are imposed. In the walls the boundary velocity condition is calculated with the employment of laws of the wall. In this work it was setted a non dimensional distance from the wall of $y^+_{max} = 2.0$ for all the laws of the wall tested, this value was calibrated by trial and error based on the numerical estability, wich is the usual procedure for the use of these laws of the wall. In the outlet is imposed a null pressure condition. Figure 1 shows the calculation domain with the boundary conditions employed in this test case.

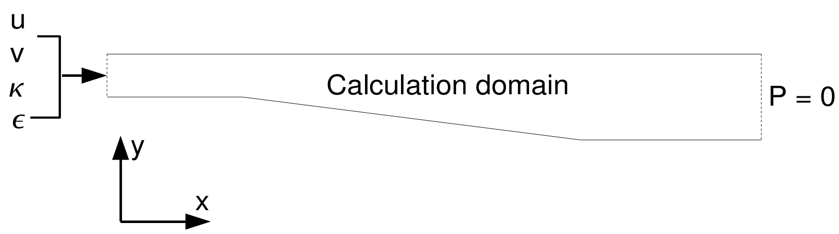

Figure 1. Calculation domain and boundary conditions- Buice and Eaton (1995) test case

The meshes used to execute the simulations are shown in Fig. 2.

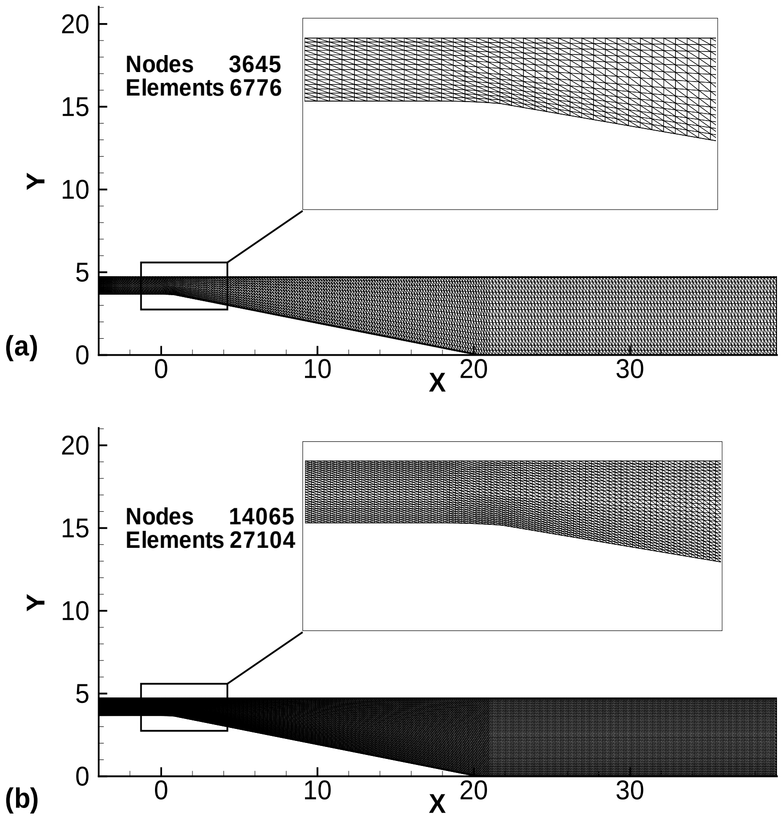

Figure 2. P1 mesh (a) and P1-isoP2 mesh (b) - Buice and Eaton (1995) test case

It is possible to notice a higher refinement level in the near wall regions. Figure 2 b indicates that the P1-isoP2 mesh contains 27,104 elements. This is a considerable fine mesh for this kind of phenomenon. Figure 3 shows the difference in the inlet detail considered in this work. This means that all the simulations were executed considering a sharp and a smooth transition in the inlet and in the outlet of the diffuser.

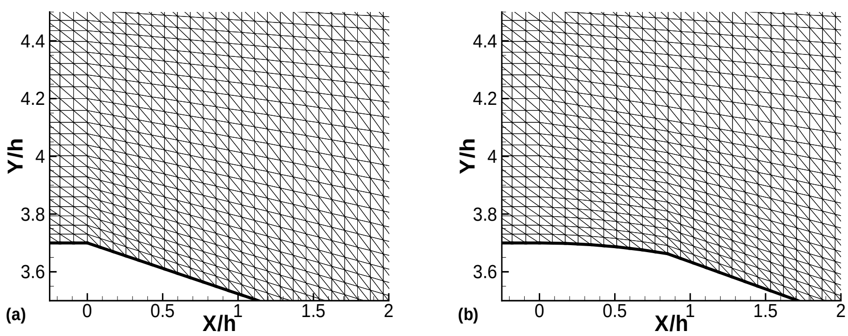

Figure 3. Sharp transition (a) and smooth transition (b) - Buice and Eaton (1995) test case

The velocity profiles obtained numerically with the use of the four laws of the wall considered were taken in eight points, illustrated in Fig. 4.

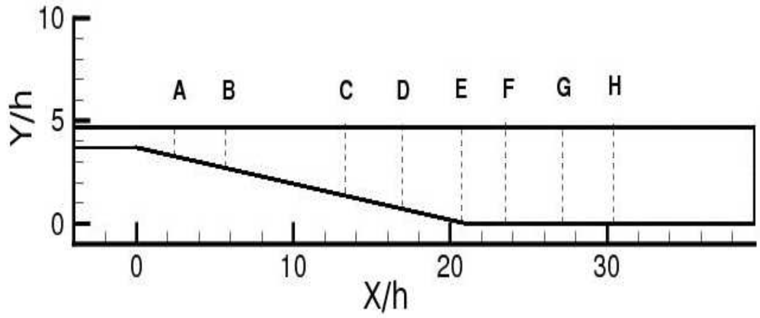

Figure 4. Points where the profiles were taken - Buice and Eaton (1995) test case

Figure 5 shows the profiles taken in points A,B,C and D.

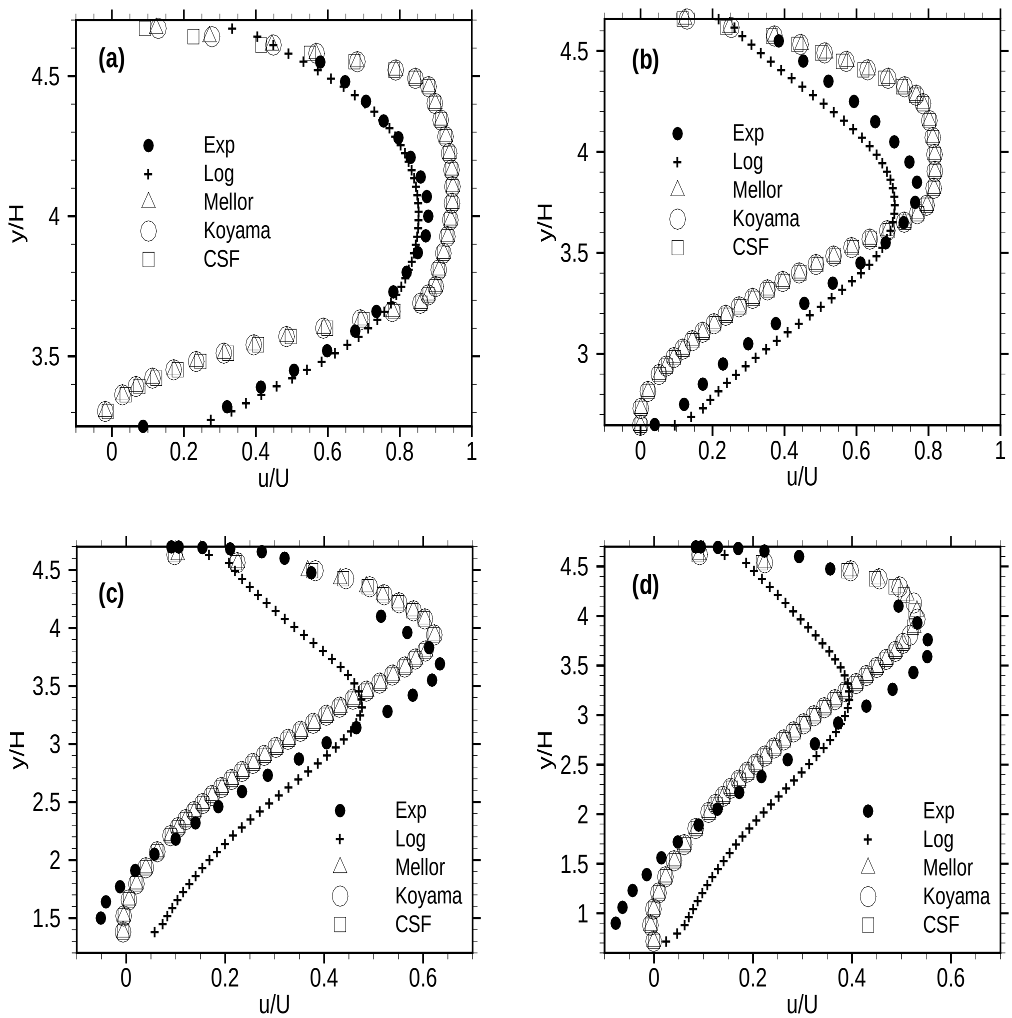

Figure 5. Velocity profiles in points A (a), B (b) C (c) and D (d) - Buice and Eaton (1995) test case

It is possible to observe that the classic log law of the wall reproduces better the dynamic behavior of the flow before de detachment point, in profiles A and B. Point C represents the detachment point. From this point until the end of the test section, the three laws of the wall that consider the existing pressure gradient action are those that better reproduces the flow behavior, with little difference between then. Figure 6 illustrates the velocity profiles taken from point E to point H.

It is importante to notice that at the last measurement section, the numerical profiles obtained with the use of the laws of the wall of Mellor (1966), Nakayama and Koyama (1984) and Cruz e Silva Freire (1998) generates a very good agreement between numerical and experimental results.

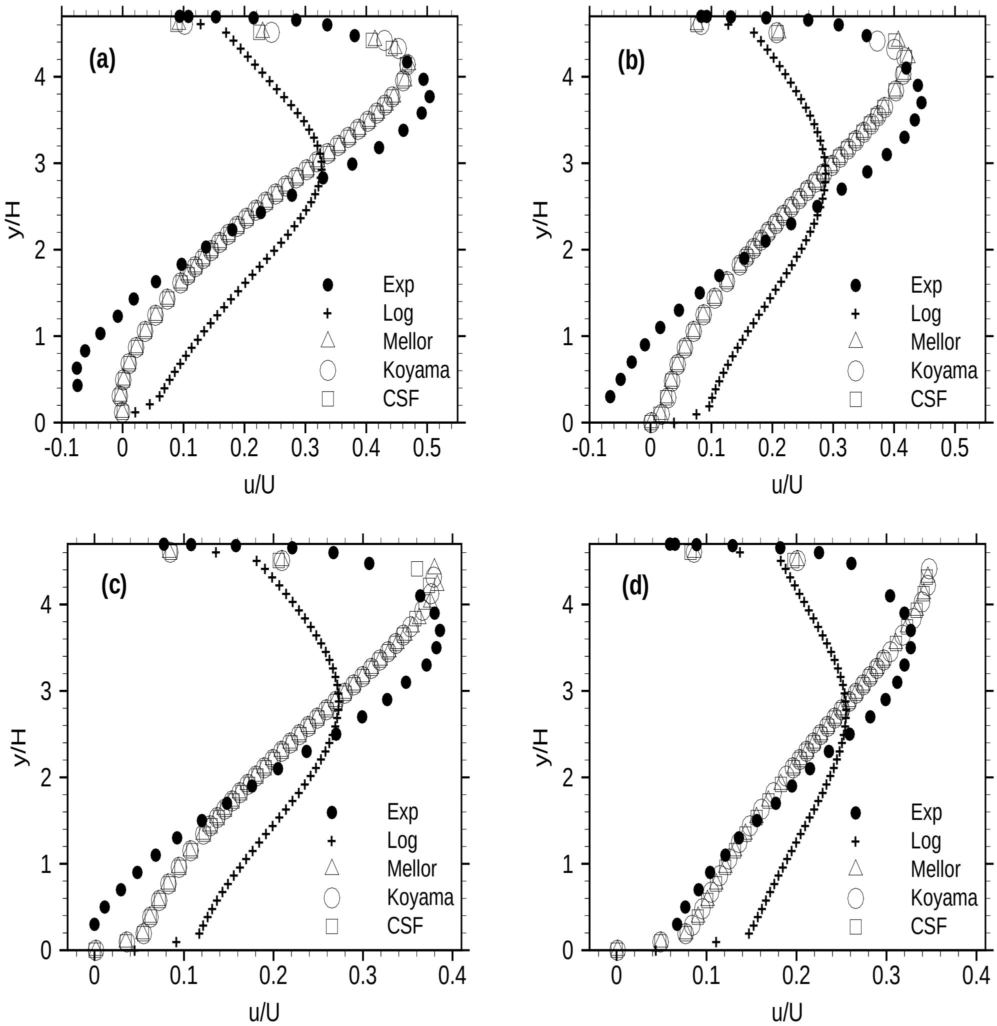

Figure 6. Velocity profiles in points E (a), F (b) G (c) and H (d) - Buice and Eaton (1995) test case

It is interesting to notice that in this case the log law is not capable to predict the boundary layer detachment. This behavior is different from the one observed in geometries where the detachment is induced by a sudden change in the geometry, such as in a channel with square ribs simulated by Gontijo and Fontoura Rodrigues (2007), or in the backward facing step flow, as showed by Gontijo and Fontoura Rodrigues (2008).

The consideration or not, of the geometrical detail in the inlet and in the outlet of the diffuser, is not capable to produce a great change in the velocity profiles, but they influence the aspect of the recirculation region. Figure 7 shows how the geometry influences the aspect of the recirculation region when the flow field is calculated using the Mellor (1966) law of the wall. This confrontation is done for the law of the wall of Koyama and Nakayama (1984), Fig. 8, and for the law of the wall of Cruz and Silva Freire (1998), Fig. 9.

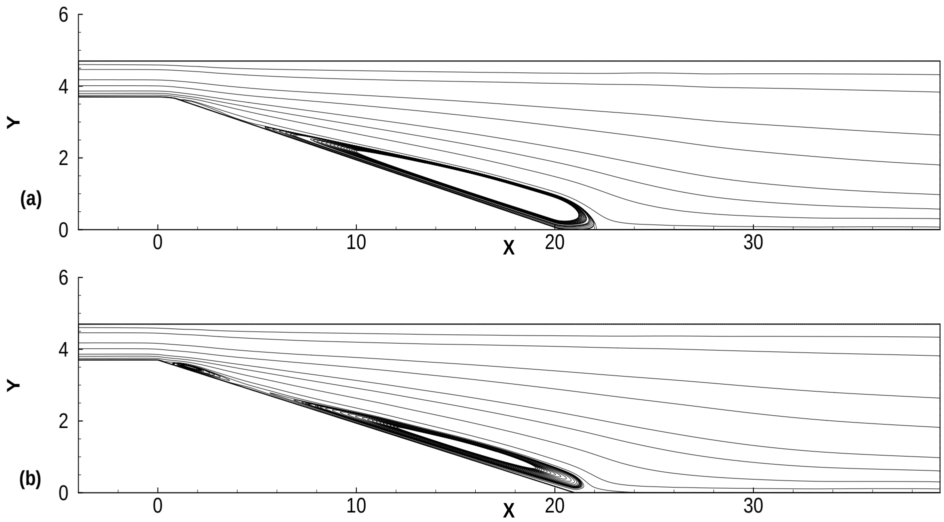

Figure 7. Smooth transition (a) and sudden change (b) - Mellor (1966) law - Buice and Eaton (1995) test case

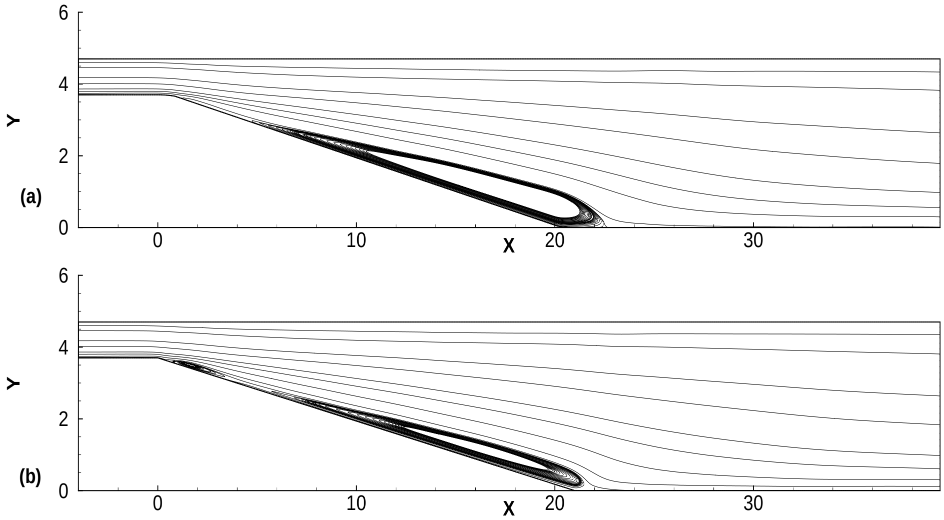

Figure 8. Smooth transition (a) and sudden change (b) - Koyama and Nakayama (1984) law - Buice and Eaton (1995) test case

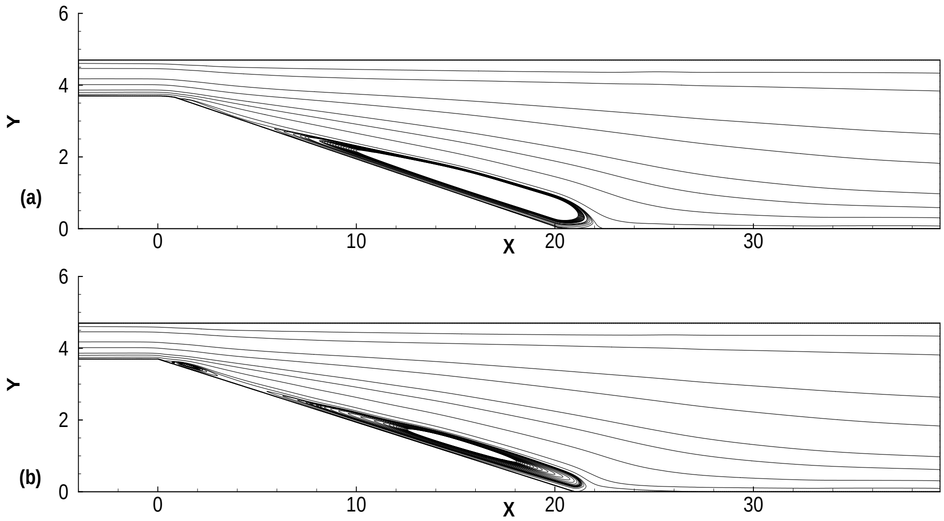

Figure 9. Smooth transition (a) and sudden change (b) - Cruz and Silva Freire (1998) law - Buice and Eaton (1995) test case

The behavior obtained with all laws of the wall is consistent. This means that, for this divergence angle, the sudden change in the geometry acts like a micro vortex generator, that injects energy in the turbulent boundary layer and creates a localized smaller recirculation region. This result is interesting because it shows a simple manner to minimize that waste of energy spent in the recirculation region, just by not considering a smooth transition in the inlet and in the outlet of the diffuser. Of course this behavior is justified by the small opening angle. If large opening angles were considered, the sharp transition in the inlet and in the outlet would increase the size of the recirculation region.

5. CONCLUSIONS

This work does an analysis based on the use of laws of the wall capable to consider the existing pressure gradients in the internal region of the turbulent boundary layer and it shows two interesting facts. The first of them is that the classic log law used in most of the commercial packages that employs the high Reynolds $\kappa - \varepsilon$ model is uncapable to predict the boundary layer detachment when it is caused by a smooth adverse pressure gradient imposed by the geometry. On the other hand, the laws of Mellor (1966), Koyama and Nakayma (1984) and of Cruz and Silva Freire (1998), that consider the influence of pressure gradients in the near wall region were capable to produce a behavior very closed to the experimental measurements of Buice and Eaton (1995).

The numerical simulation of the asymmetric straight-walled diffuser, with an divergence angle of 9.97^o, discloses that the non consideration of a smooth transition, in the inlet and in the outlet of the diffuser, is capable to induce the generation of localized micro vortex that injects energy in the turbulent boundary layer, minimizing the size of the recirculation region, in a behavior similar to the addition of a roughned wall.

6. REFERENCES

Boussinesq, J., 1877, "Théorie de l'écoulement Tourbillant" , Mem. Présentés par Divers Savants Acad. Sci. Inst. Fr., vol. 23, pp. 46-50.

Buffat, M., 1981, "Formulation moindre carrés adaptées au traitement des effets convectifs dans les équation de Navier-Stokes", Doctorat thesis, Université Claude Bernard, Lyon, France.

Buice, C. and Eaton, J., 1995. "Experimental investigationof flow through an asymmet- ric plane diffuser". Annual Research Briefs - 1995, Center of Turbulence Research, Stanford University/ NASA Ames. 117-120.

Brison ,J. F., Buffat, M., Jeandel,D., Serrer,E., 1985, "Finite elements simulation of turbulent flows, using a two equation model", Numerical methods in laminar and turbulent flows, Swansea. Pineridg Press.

Brun, G., 1988, "Developpement et application d'une methode d'elements finis pour le calcul des ecoulements turbulents fortement chauffes " , Doctorat thesis, Laboratoire de Mécanique des Fluides, Escola Central de Lyon.

Colburn, A.P., 1933 , "A method for correlating forced convection heat transfer data and a comparison with fluid friction " Transaction of American Institute of Chemical Engineers, vol. 29, pp. 174-210.

Cruz, D.O.A., Silva Freire, A.P., 1998, "On single limits and the asymptotic behavior of separating turbulent boundary layers", International Journal of Heat and Mass Transfer, vol. 41, n^o 14, pp. 2097-2111.

Favre, A., 1965, "Equations de gaz turbulents compressibles". Journal de mecanique, vol. 3 e vol. 4.

Fontoura Rodrigues, J. L. A., 1990, "Méthode de minimisation adaptée à la techinique des éléments finis pour la simulation des écoulements turbulents avec conditions aux limites non linéaires de proche paroi", Doctorat thesis, Ecole Centrale de Lyon, France.

Jones, W. and Launder, B.E., 1972, "The prediction of laminarization with a two equations model of turbulence", International Journal of Heat and Mass Transfer, vol. 15, pp. 301-314.

Kays,W.M., Crawford, M.E. 1993, "Convective Heat and Mass Transfer", McGraw Hill, INC., USA.

Launder, B.E. and Spalding, D.B., 1974, "The numerical computation of turbulent flows", Computational Methods in Applied Mechanical Engineering, vol. 3, pp. 269-289.

Mellor, G.L., 1966, "The effects of pressure gradients on turbulent flow near a smooth wall", Journal of Fluid Mechanics, vol. 24, n^o 2, pp. 255-274.

Nakayama, A., Koyama, H., 1984, "A wall law for turbulent boundary layers in adverse pressure gradients", AIAA Journal, vol. 22, n^o 10, pp. 1386-1389.

Reynolds, O., 1895, "On The Dynamical Theory of Incompressible Viscous Fluids and the Determination of the Criterium" , Philosophical Transactions of the Royal Society of London, Series A, Vol 186, p. 123.

Soares, D. V., Fontoura Rodrigues, J. L. A., 2004. "The Performance of Thermal and Velocity Wall Laws". ENCIT 2004, 10th Brazillian Congress of Thermal Sciences and Engineering, November 29 - December 03, 2004, Rio de Janeiro, Brasil.

7. Responsibility notice

The author(s) is (are) the only responsible for the printed material included in this paper